



Selection of straw waste reinforced sustainable polymer composite using a multi-criteria decision-making approach

Tej Singh¹ · Imre Fekete² · Sándor Kálmán Jakab² · László Lendvai²

Received: 30 January 2023 / Revised: 23 March 2023 / Accepted: 24 March 2023
© The Author(s) 2023

Abstract

The valorization of straw waste as a sustainable and eco-friendly resource in polymer composites is critical for resource recycling and environmental preservation. Therefore, many research works are being carried out regarding the development of wheat straw-based polymer composites to identify the reinforcing potential of these sustainable resources. In this study, three different sizes of wheat straw fibers (60–120 mesh, 35–60 mesh, and 18–35 mesh) were used, and their different ratios (0, 2.5, 5, 10, and 20% by weight) were systematically investigated for the physical and mechanical properties of polypropylene-based sustainable composites. The results indicated that the evaluated composites' properties are strongly dependent on the quantity and size of the utilized wheat straw. Therefore, a preference selection index was applied to rank the developed sustainable polymer composites to select the best composition. Various properties of the composite materials were considered as criteria for ranking the alternatives, namely tensile strength and modulus, flexural stress at conventional deflection and flexural modulus, impact strength, density, water absorption, material cost, and carbon footprint. The decision-making analysis suggests the alternative with wheat straw content of 20 wt.% (35–60 mesh size) dominating the performance by maximizing the beneficial criteria and minimizing the non-beneficial criteria, making it the most suitable alternative. This study will significantly help formulation designers to deal with the amount and size issues when developing polymeric composites.

Keywords Natural fiber · Sustainable composites · Wheat straw · Polypropylene · Multi-criteria decision-making · Preference selection index

1 Introduction

By 2050, worldwide grain output must rise by almost 50% to meet the rising demand, which will result in increased harvesting waste generation [1]. According to statistics, agricultural waste is generated annually in excess of 2.9 billion tons globally [2]. One of the most frequently produced crops in the world, wheat, is grown in 122 countries, and under a variety of environmental conditions (<https://worldpopulationreview.com/country-rankings/>

[wheat-production-by-country](#)). For 2021/2022, the global wheat output reached 778.6 million tons, with the quantity of generated wheat residues (e.g., stubble, straw) predicted to be about one billion tons [2] (https://www.statista.com/topics/1668/wheat/#topicHeader__wrapper). The handling of waste wheat straw (WS) is an urgent and challenging social concern. A portion of the WS produced is utilized as animal feed, agricultural fertilizer, mushroom compost, and a source of bio-energy [3, 4]. However, despite the fact that burning WS has been outlawed by a number of nations, considerable amounts of straw are still burnt openly [5]. The open-air combustion of straw waste can produce a substantial quantity of particulate matter, and toxic gases, such as nitrides, sulfur, methane, carbon dioxide, and carbon monoxide, resulting in severe air pollution [3–5]. The burning of straw waste in the field also endangers highway, railway, and aviation traffic safety and gravely harms human health and security [2]. Therefore, a novel strategy to transform WS into a useful end product is urgently required

✉ László Lendvai
lendvai.laszlo@sze.hu

¹ Savaria Institute of Technology, Eötvös Loránd University, 9700 Szombathely, Hungary

² Department of Materials Science and Engineering, Széchenyi István University, 9026 Győr, Hungary

to lessen its detrimental effects on the environment. It is notable that the global market for WS, which was predicted to be worth 643.6 million USD in 2021, is expected to increase to 1330.24 million USD by 2029, with a forecasted compound annual growth rate of 9.5% from 2022 to 2029 (<https://www.databridgemarketresearch.com/reports/global-wheat-straw-market>). Therefore, utilizing WS in new, eco-friendly ways to make products and materials makes it a great zero-waste alternative.

Currently, considerable efforts are being devoted to replacing petrochemical plastics using vegetable-based polymeric materials, such as biopolymers [6] and natural fiber-filled composites [7]. These latter integrate the vegetable fillers — including straw — with polymers and enable the resulting composites to be structural materials with various uses [7–9]. The demand for such materials is constantly growing. Particularly, in the automotive industry, it is an ideal approach to utilize WS as a commodity and resource.

In a recent study, the authors investigated the impact of micron-sized WS particles (0–50 phr at steps of 10 phr) on the mechanical properties of natural rubber-based composites [10]. An improvement of ~62% in tensile strength was reported for 20 phr WS-loaded natural rubber composites, which decreased with further loading. The hardness and storage modulus of the investigated composites was found to increase with increased WS-content and noted largest for 50 phr WS-loaded natural rubber composites. In another research work [11], the authors studied the effect of WS particle size and amount on the mechanical properties of polyhydroxy-co-3-butyrate-co-3-valerate (PHBV)-based composites. Three particle sizes of WS such as ~17 μm , ~109 μm , and ~469 μm were selected and varied from 0 to 30 wt.% in the PHBV matrix. The strain, stress, and energy at break were found to decrease with increasing particle size and WS loading. Almost 15% enhancement in Young's modulus was noted for the composites having 20 wt.% of 17 μm -sized WS. Ahankari et al. [12] studied the effect of WS (average length = 250 μm) on the mechanical properties of PHBV and polypropylene (PP)-based composites, respectively. The amount of WS was 30 wt.% and 40 wt.% in PHBV, while it was 30 wt.% for PP. The inclusion of WS resulted in the deterioration of elongation at break, tensile, and impact strength, while a steep increment in tensile and flexural modulus was noted. Notably, a relative enhancement of almost 52% in flexural strength of PHBV composite was recorded at 30 wt.% WS-content. Meanwhile, the addition of 30 wt.% WS into the PP-based composite resulted in an almost the same flexural strength as that of neat PP. While investigating the influence of WS loading (20 wt.%) on PHBV-based composites, M.-A. Berthet et al. [13] investigated the effect of fiber moisture content of PHBV/WS composites with 20 wt.% WS content.

The authors showed that the mechanical properties are barely affected by the initial moisture content. In the research work of Mu et al. [14], various agricultural wastes, including WS (length = $588.4 \pm 418.2 \mu\text{m}$) were assessed for their influence on high-density polyethylene-based composites. The inclusion of WS resulted in a ~44%, ~332%, ~110%, and ~512% enhancement in tensile strength, Young's modulus, flexural strength, and flexural modulus, respectively. Ming-Zhu Pan et al. [15] studied the impact of WS size (9, 28, and 35 mesh) and content (0–50 wt.% at steps of 10 wt.%) on the mechanical properties of PP-based composites. The Young's modulus, tensile, and flexural strength of the composites increased linearly with increasing WS content up to 40%. Compared with the composites prepared with the longer WS, the composites made the finest ones (> 35 mesh) had a slightly higher tensile strength.

According to the reviewed literature, WS quantity and size have a significant influence on the ultimate performance of such polymer composites. Because of its good strength-to-weight ratio, low cost, versatility, and simplicity of processing, PP is a polymer that is widely utilized in the automobile sector, often paired with various additives, including agricultural by-products [16, 17]. Nowadays, choosing the components of binary/ternary materials in the right quantities and designing the formulation for optimal qualities are real-world issues that a researcher in the field of polymer composites must deal with. The reason for this is that each manufactured composite has its own performance for each individual characteristic. Hence, a judgment on the optimal composite with the highest degree of satisfaction for all material attributes is necessary. In these circumstances, multi-criteria decision-making (MCDM) has been regarded as a reliable and quick decision-making tool. MCDM techniques are prospective quantitative ways to solve decision issues with a finite number of alternatives and criteria (that are material properties) [18, 19]. Over the past years, several researchers have investigated the problem of polymer composite selection optimization with different techniques, including AHP, ARAS, TOPSIS, MAIRCA, WASPAS, MABAC, MEW, MOORA, and VIKOR, to name a few [20–27]. The criteria weight affects the alternative rankings in most of these techniques that are hard to understand and difficult to apply since they need much mathematical expertise. The preference selection index (PSI) technique is simpler to understand than any other MCDM method since there is no consideration of the relative relevance of the criteria, and the total preference value is determined by using the statistical notion [28]. The exquisiteness of the PSI technique is that it is useful in evaluating optimal alternatives when there is disagreement about the relative relevance of the criteria, and it also requires less numerical calculations. The PSI technique was prosperously utilized in the ranking of polyamides by

Haoues et al. [25], in the selection of ship body materials by Gangwar et al. [29], in the selection of materials for marine applications by Yadav et al. [30], optimizing solar air heater parameters by Chauhan et al. [31], ranking barriers to green human resource management implementation by Tweneboza Kodua et al. [32] and in several other studies too [33, 34].

The current paper explores the effects of adding waste WS at various weight percentages and sizes to PP composites by evaluating their physico-mechanical characteristics. In the present study, a series of PP-based composites with varying concentrations (0, 2.5, 5, 10, and 20% by weight) of different sized (60–120 mesh, 35–60 mesh, and 18–35 mesh) waste WS has been designed, fabricated, and assessed for various properties (density, hardness, impact strength, tensile strength, flexural stress at conventional deflection, tensile modulus, flexural modulus, material cost, and carbon footprint). According to the best knowledge of the authors, no previous studies dealt with using MCDM techniques for the evaluation of such composite materials. Therefore, the PSI approach has been used to select the best possible alternative among the fabricated composites.

2 Materials and methods

2.1 Materials

The PP used as matrix material in this work was a commercial product of MOL Petrochemicals Co. Ltd. under the trade name TIPPLEN H145F. It is an injection molding grade

polymer with a melt flow rate of 29 g/10 min (measured at 230 °C and 2.16 kg load). The WS used as filler was kindly provided by Mikó Stroh Borotai-Laska Ltd. The straw fibers were washed with distilled water, then dried, ground, and sieved. The ground fibers were separated into three fractions to analyze the influence of particle size on the properties of PP/WS composites. The shortest fraction consisted of WS particles collected from between the sieves of 60 and 120 mesh (125–250 µm). The intermediate group was obtained from the sieves between 35 and 60 mesh (250–500 µm), while the largest ones from between 18 and 35 mesh (500–1000 µm). Composites with 10 wt.% WS content were prepared from the different-sized straws, while the effect of WS concentration was also analyzed by fabricating samples of 0–20 wt.% straw content, using the fibers with a size between 60 and 120 mesh. Optical microscopic images of the different WS fractions are shown in Fig. 1. No chemicals or any further additives were incorporated into the prepared composites.

2.2 Composite fabrication

The components of the fabricated composites were dried for 6 h before melt compounding at 80 °C using a Faithful WGLL-125BE model drying chamber. Subsequently, they were fed into a Labtech LTE 20–44 twin-screw extrusion machine with a barrel of increasing temperature (160 to 180 °C). The extrusion rotational speed was set to 40 /min. The designation and the composition of the prepared samples are collected in Table 1.

Fig. 1 Optical microscopic images of wheat straws with a size of **a** 60–120 mesh, **b** 35–60 mesh, and **c** 18–35 mesh

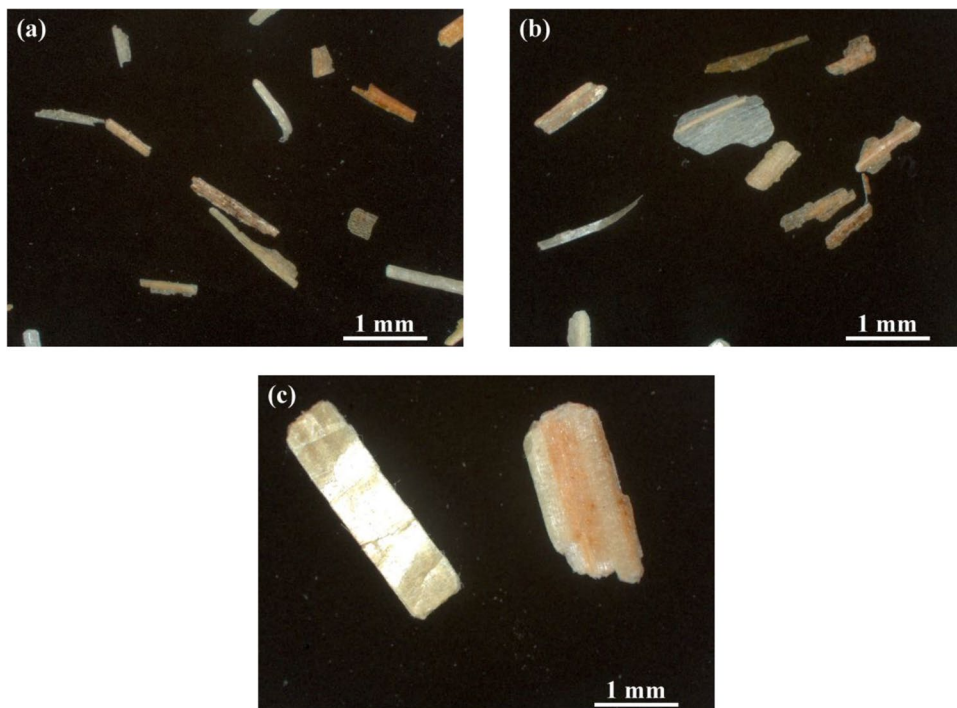
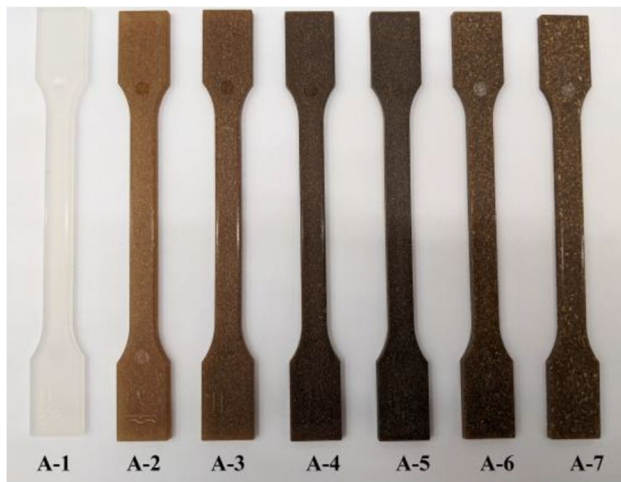


Table 1 The designation and composition of the fabricated samples

Designation	PP content [wt.%]	Wheat straw content [wt.%]	Wheat straw size
A-1	100	0	-
A-2	97.5	2.5	60–120 mesh
A-3	95	5	60–120 mesh
A-4	90	10	60–120 mesh
A-5	80	20	60–120 mesh
A-6	90	10	35–60 mesh
A-7	90	10	18–35 mesh

**Fig. 2** Photographic image of the prepared specimens

Injection molding of dogbone-shaped specimens was carried out with an Arburg Allrounder 420C type injection molding machine. The barrel of the injection unit was heated with increasing heating sections from the feeder to the nozzle in the temperature range of 170–200 °C. The nozzle was heated up to 210 °C, while the mold was kept at 25 °C. The injection rate was set to 30 cm³/s. The injection pressure was set to 1000 bar, while the holding pressure was 750, 650, and 250 bar. Examples of the prepared specimens with their designations are shown in Fig. 2.

2.3 Characterization

Tensile properties were determined according to ISO 527, while the flexural properties were according to the ISO 178 standard. Both measurements were carried out with an Instron 5582 universal testing machine equipped with a 10 kN load cell. The theoretical cross-section of the samples was 10×4 mm²; however, each specimen was measured individually with a caliper, and the measured values were used for strength and modulus calculations. During the tensile test, the initial gripped length

of the specimens was 100 mm. The crosshead speed was 1 mm/min for the measurement of the modulus and 25 mm/min for the general testing. For the flexural test, the machine was equipped with a 3-point bending setup of 64 mm span length. Likewise, 1 mm/min initial crosshead speed was used for determining the modulus, which was increased to 5 mm/min. The results reported for both tensile and flexural tests are the averages of five parallel measurements carried out at ambient temperature.

Charpy impact test was performed according to the ISO 179 standard with a Ceast 6545 impact testing device. The tests were executed on un-notched, rectangular specimens (10×4 mm² cross-section and 80 mm length), with a span length of 62 mm. A 15 J pendulum hammer was used as a measuring tool. The results reported are the averages of five parallel measurements carried out at ambient temperature.

Water absorption of the samples was tested by immersing them in distilled water. Specimens were prepared for water absorption test by drying them overnight at 80 °C in advance. The absorption test was performed for 30 days. The weight of the composite specimens was measured right before the immersion and after 30 days. The percentage-based water uptake (M_t) of the specimens was calculated according to Eq. 1:

$$M_t[\%] = \frac{W_w - W_d}{W_d} * 100 \quad (1)$$

where W_w is the weight of the specimens after 30 days, and W_d is their initial dry weight. The results reported are the averages of three parallel measurements.

The density of the fabricated samples was determined by measuring the weight of samples of known volume (~10×10×4 mm³). The exact volume size of each specimen was validated by computed tomographic (CT)-based 3D scans of high accuracy. The results reported are the averages of three parallel measurements.

The developed composites were further analyzed for their carbon footprint and price. Carbon footprint is a useful indicator for determining how any material or product activity affects the environment. The carbon footprint of PP and WS is taken into account in this study. Price (€/kg) was related to the cost of the PP and WS used to develop the composite.

Analysis of variance (ANOVA) and Tukey's honestly significant difference (HSD) test at a significance level of 5% ($p < 0.05$) were used to statistically evaluate the data obtained through the measurements.

3 Results and discussion

3.1 Criteria interpretation

The results of WS loading and size on the performance of each analyzed attribute are presented in Table 2. Table 2 consists of

the seven composite alternatives (A-1 to A-7, as described in Table 1) and nine properties (tensile strength, Young’s modulus, flexural stress at conventional deflection, flexural modulus, impact strength, density, material price, water absorption, and carbon footprint).

The tensile and flexural mechanical properties of PP/WS composites are depicted in Fig. 3a. The tensile strength of unfilled PP (A-1) and its composites containing 2.5 wt.% (A-2), 5 wt.% (A-3), 10 wt.% (A-4), and 20 wt.% (A-5) WS of 60–120 mesh are 30.7 MPa, 29.2 MPa, 29.1 MPa, 27.6 MPa, and 26.1 MPa, respectively. This indicates a notable decrement in tensile strength with the increasing amount of WS filler. Similar trends have already been reported in the literature for WS-containing polymer composites [35] and are generally attributed to the poor adhesion between the components. The limited interaction between PP and the straw particles can be explained by the differences in polarity. While PP is a non-polar material, WS is greatly polar due to the numerous -OH groups on its surface. Throughout the last decades, numerous studies have been devoted to overcoming this issue by introducing additional chemicals as coupling agents, thereby improving compatibility. These measures, however, greatly

reduce the “green” characteristics of the developed materials, making them less environmentally friendly. About the size of the WS, it can be concluded, that using the smaller particles generally led to higher strength. The lowest strength was exhibited by composites filled with straw particles of 18–35 mesh (sample A-7: 26.2 MPa), while the highest one remained for the 60–120 mesh-sized WS containing sample (sample A-4: 27.6 MPa).

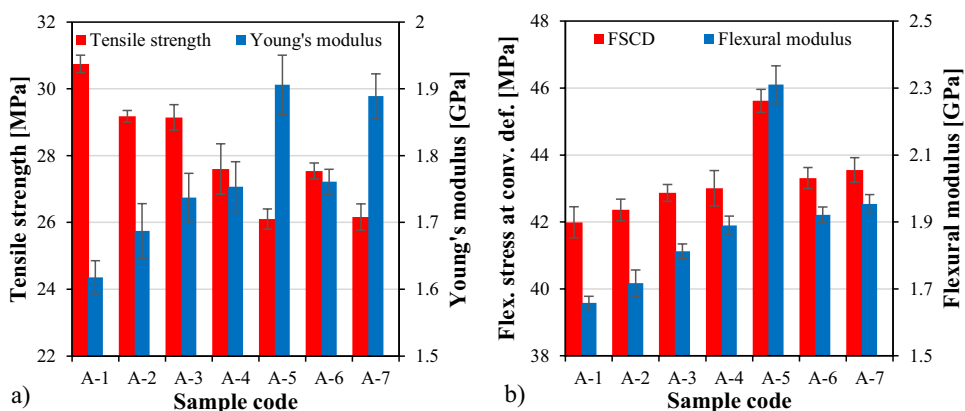
Contrary to the tensile strength, Young’s modulus values of the WS-containing composites were markedly improved in comparison with PP. More specifically, sample A-1 exhibited the poorest modulus of 1.62 GPa, while it gradually improved with increasing WS loading to 1.69 GPa, 1.74 GPa, 1.75 GPa, and 1.91 GPa for samples A-2, A-3, A-4, and A-5, respectively. This is not unexpected in view of the fact that the modulus of WS greatly exceeds that of PPs. According to the literature, the modulus of the WS crop straw cell wall exceeds 20 GPa [36]. Besides, unlike the tensile strength, the modulus is generally not influenced by the interphase bonding quality between the components for the reason that in the early stage of the measurement — where the modulus is calculated — there is barely any deformation present. These results are in good accord with previous

Table 2 Experimental data of the prepared samples. The used designations are the following: A-1: PP, A-2: PP+WS (2.5wt.%, 60–120 mesh), A-3: PP+WS (5wt.%, 60–120 mesh), A-4: PP+WS (10wt.%, 60–120 mesh), A-5: PP+WS (20wt.%, 60–120 mesh), A-6: PP+WS

(10wt.%, 35–60 mesh), A-7: PP+WS (10wt.%, 18–35 mesh). Different letters in the superscripts ^(a,b,c,d,e) indicate significant differences between the composites according to Tukey’s HSD test

Designation	Tensile strength [MPa]	Young’s modulus [GPa]	Flex. str. at conv. def. [MPa]	Flexural modulus [GPa]	Impact strength [kJ/m ²]	Density [g/cm ³]	Water uptake [%]	Carbon footprint [-]	Material price [€/kg]
A-1	30.8 ± 0.3 ^a	1.62 ± 0.02 ^a	42.0 ± 0.5 ^a	1.66 ± 0.02 ^a	56.9 ± 6.2 ^a	0.90 ± 0.00 ^a	0.08 ± 0.04 ^a	5 (VH)	1.2
A-2	29.2 ± 0.2 ^b	1.69 ± 0.04 ^{a,b}	42.4 ± 0.3 ^{a,b}	1.72 ± 0.04 ^a	19.5 ± 1.1 ^b	0.91 ± 0.00 ^b	0.24 ± 0.02 ^b	4 (H)	1.18
A-3	29.1 ± 0.4 ^b	1.74 ± 0.04 ^b	42.9 ± 0.3 ^{b,c}	1.81 ± 0.02 ^b	17.7 ± 1.1 ^{b,c}	0.92 ± 0.00 ^b	0.31 ± 0.00 ^c	3 (M)	1.15
A-4	27.6 ± 0.8 ^c	1.75 ± 0.04 ^b	43.0 ± 0.5 ^{b,c}	1.89 ± 0.03 ^c	17.9 ± 1.4 ^{b,c}	0.94 ± 0.00 ^c	0.5 ± 0.02 ^d	2 (L)	1.11
A-5	26.1 ± 0.3 ^d	1.91 ± 0.04 ^c	45.6 ± 0.3 ^d	2.31 ± 0.06 ^d	15.2 ± 1.0 ^{b,c}	0.96 ± 0.00 ^d	1.3 ± 0.04 ^e	1 (VL)	1.01
A-6	27.5 ± 0.2 ^c	1.76 ± 0.02 ^b	43.3 ± 0.3 ^c	1.92 ± 0.02 ^c	14.4 ± 1.8 ^{b,c}	0.94 ± 0.00 ^c	0.52 ± 0.05 ^d	2 (L)	1.11
A-7	26.2 ± 0.4 ^d	1.89 ± 0.03 ^c	43.6 ± 0.4 ^c	1.95 ± 0.03 ^c	12.8 ± 2.3 ^c	0.93 ± 0.00 ^c	0.56 ± 0.0 ^d	2 (L)	1.11

Fig. 3 Variation of **a** tensile strength; tensile modulus and **b** flexural stress at conventional deflection; flexural modulus. The used designations are the following: A-1: PP, A-2: PP+WS (2.5wt.%, 60–120 mesh), A-3: PP+WS (5wt.%, 60–120 mesh), A-4: PP+WS (10wt.%, 60–120 mesh), A-5: PP+WS (20wt.%, 60–120 mesh), A-6: PP+WS (10wt.%, 35–60 mesh), A-7: PP+WS (10wt.%, 18–35 mesh)



studies published on the topic of natural fiber-reinforced polymer composites including the ones with polyolefin matrices [12, 37].

PP is a highly ductile material, as such it barely tends to break under 3-point bending circumstances at ambient temperature and above. For materials of this kind, the corresponding standards (ISO 178 and ASTM D790) prescribe the flexural stress at conventional deflection (FSCD) to be reported instead of flexural strength in order to eradicate the effect of slipping of the specimen during the bending. Accordingly, in this study, the stress values at the conventional deflection (3.5%) were evaluated, following the ISO 178 standard. As Fig. 3b shows, the FSCD of the prepared samples gradually improves with increasing filler content. The FSCD value of sample A-1 (virgin PP) increased from the initial 42.0 up to 45.6 MPa when 20 wt.% straw was incorporated into it (sample A-5). This is exactly the opposite of what was observed during the tensile tests. The explanation for this contradiction is twofold. Firstly, since the WS particles tend to increase the stiffness of the polymer matrix (see modulus values), the initial region of the stress–strain curves tends to be steeper, resulting in higher stress values at the conventional limit of 3.5%, unless the fillers are deteriorating the mechanical properties of the polymer matrix so much that it breaks before reaching the conventional deflection. Apparently, WS was a proper filler from this aspect, since early failure did not occur. Secondly, 3-point bending exposes specimens to a special kind of load, where tension and compression are combined. Filled polymer systems generally tend to perform better against compressive forces than tensile ones, which might also explain the improved FSCD values of the PP/WS composites against the virgin PP. Similar observations have already been shown for polymer composites of various matrices [26].

Overall, the flexural modulus values of all composites were enhanced compared to sample A-1 (1.66 GPa). In this regard, sample A-5 with its 20 wt.% of WS showed to be superior against all the other composites with a modulus of 2.31 GPa, which is relatively ~40% higher than that of A-1. This is in good agreement with the tensile tests' results, and

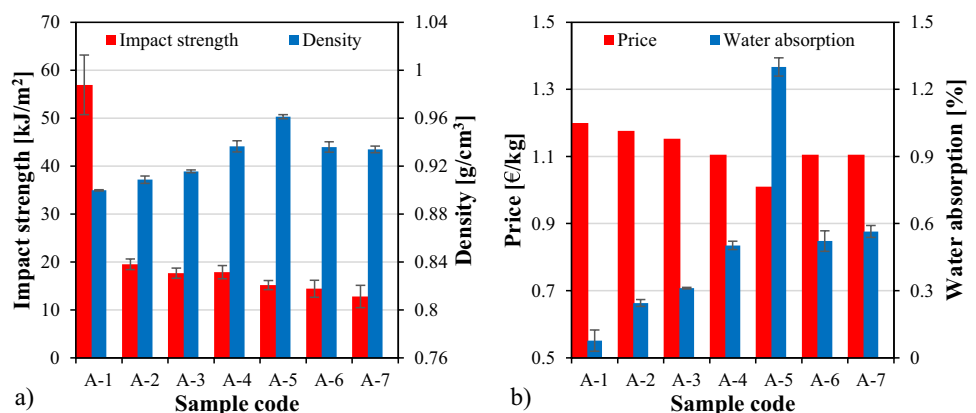
it can be attributed to the rigid characteristics of the straw particles used as filler materials in this study.

Unlike the tensile and flexural properties, the impact behavior of the PP deteriorated drastically when WS particles were incorporated into it, even in the lowest amount (Fig. 4a). While the initial impact strength of neat PP (sample A-1) was ~57 kJ/m², it dropped to ~20 kJ/m² for sample A-2, even though the filler content was only 2.5 wt.%. Lignocellulosic particles, such as straw, are considered rigid organic fillers, and as such, they tend to decrease the toughness of the polymer matrices markedly [38]. Combining this brittle characteristic of WS with the poor interfacial adhesion between the components explains this immense drop in impact resistance. For composites with further WS content, only a slight decrease was observed, bottoming at ~13 kJ/m² for sample A-7 (10 wt.% WS of 18–35 mesh particle size).

The density of the fabricated samples is presented in Fig. 4a. While PP-s of various grades tend to have a stable density (0.9 g/cm³), for organic particles like WS, the bulk density is reported to be greatly varying and depends on multiple factors (porosity, size, origin, etc.) [39]. In this current study, the density of the particles was determined to be 1.49 g/cm³, 1.47 g/cm³, and 1.43 g/cm³ for the particles of 60–120 mesh, 35–60 mesh, and 18–35 mesh, respectively. The decreasing density with increasing particle size can be attributed to the greater porosity in the larger particles. Overall, the density of the filler fractions was similar, and all of them exceeded that of PPs. Considering this fact, obviously, sample A-1 exhibited the lowest density (0.9 g/cm³), and it gradually increased with higher WS content, peaking at 0.96 g/cm³ for sample A-5 (20 wt.% WS).

The water uptake of PP and the PP/WS composites after 30 days of immersion in distilled water is shown in Fig. 4b. Based on the diagram, it can be safely assumed that absorbed water is continuously increasing with increasing straw content. The higher water uptake of the WS-containing samples can be attributed to the large

Fig. 4 Variation of **a** impact strength; density and **b** material price; water absorption. The used designations are the following: A-1: PP, A-2: PP + WS (2.5wt.%, 60–120 mesh), A-3: PP + WS (5wt.%, 60–120 mesh), A-4: PP + WS (10wt.%, 60–120 mesh), A-5: PP + WS (20wt.%, 60–120 mesh), A-6: PP + WS (10wt.%, 35–60 mesh), A-7: PP + WS (10wt.%, 18–35 mesh)



number of –OH groups on the straw fibers’ surface that formed hydrogen bonds with the water molecules, thereby promoting the absorption. Additionally, straw particles tend to have a cellular structure, where water can penetrate through capillarity; thereby, it also contributes to the overall water uptake of the composites [40]. Comparing the samples with identical straw content of different sizes (A-4, A-6, A-7), it can be assumed that the composite samples with larger particles generally absorbed slightly more water referring to more voids in these fibers.

The price of composite A-1 is the highest (1.20 €/kg) as it contains the cost of PP. With the inclusion of WS, the price of the composites decreased due to its lower cost (0.25 €/kg) and remained lowest for A-5 composite with 20 wt.% WS content. A five-point scale (Table 2) has been considered for carbon footprint as 1, very low (VL); 2, low (L); 3, medium (M); 4, high (H); and 5, very high (VH). The carbon footprint for alternative A-1 containing PP was VH (5), while for alternative A-5, it was VL (1). The carbon footprint of PP (~1.34 kg CO₂-eq/kg) is much higher compared to WS (~0.14 kg CO₂-eq/kg) [41, 42].

It is clear from Table 2 and Figs. 3 and 4 that changes in WS loading significantly affect the evaluated properties. No single composite sample performed best concerning all properties at a time. For example, composite sample A-1 exhibited the highest tensile strength, impact strength, and lowest density and water absorption. However, it showed the worst performance for tensile modulus, flexural modulus, carbon footprint, and price. In addition, the carbon footprint, price, flexural stress at conventional deflection, and flexural modulus of A-5 were superior to all composite samples but displayed the worst performance for density, water absorption, and tensile strength. Therefore, to choose the best candidate that satisfies all these conflicting properties at a time, these composite samples were ranked using the PSI-based MCDM approach. The performance criteria used in the ranking were selected as C-1 (tensile strength, higher-is-good), C-2 (Young’s modulus, higher-is-good), C-3 (flexural stress at conventional deflection, higher-is-good), C-4 (flexural modulus, higher-is-good), C-5 (impact strength, higher-is-good), C-6 (density, lower-is-good), C-7 (water absorption, lower-is-good), C-8 (carbon footprint, lower-is-good), and C-9 (price, lower-is-good).

3.2 Proposed MCDM methodology

The PSI technique proposed by Maniya and Bhatt [28] uses the overall preference value to assign an index rating to each alternative, and the alternative with the higher index value is selected as the best option. Figure 5 depicts the MCDM methodology adopted to rank the alternatives of the WS-filled PP composites.

The detailed steps for the PSI method are given as follows:

Step 1: Decision matrix $([\delta_{ij}]_{n \times m})$ construction.

For n alternatives ($A_i, i = 1, 2, \dots, n$) and m criteria ($C_j, j = 1, 2, \dots, m$), the decision matrix is structured as:

$$[\delta_{ij}]_{n \times m} = \begin{matrix} & \begin{matrix} C_1 & C_2 & \dots & C_j & \dots & \delta_m \end{matrix} \\ \begin{matrix} A_1 \\ A_2 \\ \vdots \\ A_1 \\ \vdots \\ A_n \end{matrix} & \begin{vmatrix} \delta_{11} & \delta_{12} & \dots & \delta_{1j} & \dots & \delta_{1m} \\ \delta_{21} & \delta_{22} & \dots & \delta_{2j} & \dots & \delta_{2m} \\ \vdots & \vdots & \dots & \vdots & \dots & \vdots \\ \delta_{11} & \delta_{i2} & \dots & \delta_{ij} & \dots & \delta_{im} \\ \vdots & \vdots & \dots & \vdots & \dots & \vdots \\ \delta_{n1} & \delta_{n2} & \dots & \delta_{nj} & \dots & \delta_{nm} \end{vmatrix} \end{matrix} \quad (2)$$

Here, δ_{ij} = i th alternative performance based on j th criteria.

Step 2: Normalized decision matrix $([\delta n_{ij}]_{n \times m})$ construction.

The structured decision matrix $([\delta_{ij}]_{n \times m})$ is normalized using Eq. 3 as follows:

$$[\delta_{ij}]_{n \times m} = \begin{cases} \frac{\delta_{ij}}{\delta_{ij}^{\max}} & \text{if } j \in \text{beneficial criteria} \\ \frac{\delta_{ij}^{\min}}{\delta_{ij}} & \text{if } j \in \text{non-beneficial criteria} \end{cases} \quad (3)$$

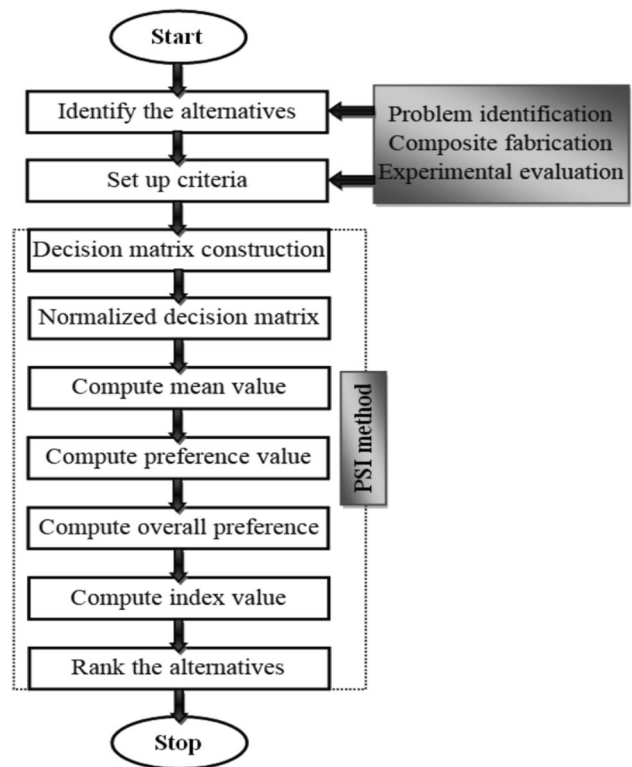


Fig. 5 Algorithm of the used PSI methodology

Step 3: Mean of the normalized value of criteria (\mathfrak{R}_j)

The mean of the normalized value of criteria (\mathfrak{R}_j) is determined using the following equation (Eq. 4):

$$\mathfrak{R}_j = \frac{1}{n} \sum_{i=1}^n \delta n_{ij}; j = 1, 2, \dots, m \tag{4}$$

Step 4: Derive the preference variation value ($\mathfrak{R}v_j$)

The preference variation value ($\mathfrak{R}v_j$) is derived for each criterion using Eq. 5 as follows:

$$\mathfrak{R}v_j = \sum_{i=1}^n [\delta n_{ij} - \mathfrak{R}_j]^2; j = 1, 2, \dots, m \tag{5}$$

Step 5: Compute the deviation (η_j) in $\mathfrak{R}v_j$ using the following equation (Eq. 6):

$$\eta_j = 1 - \mathfrak{R}v_j; j = 1, 2, \dots, m \tag{6}$$

Step 6: Determine the overall preference value (Ψ_j) using η_j as follows (Eq. 7):

$$\Psi_j = \frac{\eta_j}{\sum_{j=1}^m \eta_j}; j = 1, 2, \dots, m \tag{7}$$

Step 7: Compute the index value (Φ_i) as given in Eq. 8:

$$\Phi_i = \sum_{j=1}^m (\delta n_{ij} \times \Psi_j); i = 1, 2, \dots, n \tag{8}$$

Step 8: Assign rank to the alternatives as per the descending order of index value.

3.3 Assessment of composites using PSI methodology

The present study considered 7 composite alternatives (i.e., $n=7$) and 9 assessment criteria (i.e., $m=9$). A decision matrix $[\delta_{ij}]_{n \times m}$ is constructed for seven rows and nine columns as:

$$[\delta_{ij}]_{7 \times 9} = \begin{vmatrix} 30.75 & 1.62 & 41.99 & 1.66 & 56.93 & 0.90 & 0.08 & 5 & 1.2 \\ 29.18 & 1.69 & 42.36 & 1.72 & 19.51 & 0.91 & 0.24 & 4 & 1.18 \\ 29.14 & 1.74 & 42.87 & 1.81 & 17.67 & 0.92 & 0.31 & 3 & 1.15 \\ 27.60 & 1.75 & 43.01 & 1.89 & 17.87 & 0.94 & 0.50 & 2 & 1.11 \\ 26.10 & 1.91 & 45.62 & 2.32 & 15.17 & 0.96 & 1.30 & 1 & 1.01 \\ 27.54 & 1.76 & 43.31 & 1.92 & 14.41 & 0.94 & 0.52 & 2 & 1.11 \\ 26.16 & 1.89 & 43.55 & 1.95 & 12.80 & 0.93 & 0.56 & 2 & 1.11 \end{vmatrix}$$

After constructing the decision matrix, the maximum and minimum values for the selected nine criteria were determined.

$$[\delta_{ij}^{\max}]_9 = \begin{vmatrix} 30.75 & 1.91 & 45.62 & 2.32 & 56.96 & 0.96 & 1.30 & 5 & 1.20 \end{vmatrix}$$

$$[\delta_{ij}^{\min}]_9 = \begin{vmatrix} 26.10 & 1.62 & 41.99 & 1.66 & 12.80 & 0.90 & 0.08 & 1 & 1.01 \end{vmatrix}$$

Next, the normalized decision matrix ($[\delta n_{ij}]_{7 \times 9}$) was constructed using Eq. 3.

$$[\delta n_{ij}]_{7 \times 9} = \begin{vmatrix} 1.000 & 0.848 & 0.920 & 0.716 & 1.000 & 1.000 & 1.000 & 0.200 & 0.842 \\ 0.949 & 0.885 & 0.929 & 0.741 & 0.343 & 0.989 & 0.333 & 0.250 & 0.856 \\ 0.948 & 0.911 & 0.940 & 0.780 & 0.310 & 0.978 & 0.258 & 0.333 & 0.878 \\ 0.898 & 0.916 & 0.943 & 0.815 & 0.314 & 0.957 & 0.160 & 0.500 & 0.910 \\ 0.849 & 1.000 & 1.000 & 1.000 & 0.266 & 0.938 & 0.062 & 1.000 & 1.000 \\ 0.896 & 0.921 & 0.949 & 0.828 & 0.253 & 0.957 & 0.154 & 0.500 & 0.910 \\ 0.851 & 0.990 & 0.955 & 0.841 & 0.225 & 0.968 & 0.143 & 0.500 & 0.910 \end{vmatrix}$$

After normalization, the mean of the normalized value of criteria (\mathfrak{R}_j) was computed using Eq. 4.

$$[\mathfrak{R}_j]_9 = \begin{vmatrix} 0.913 & 0.924 & 0.948 & 0.817 & 0.387 & 0.970 & 0.301 & 0.469 & 0.901 \end{vmatrix}$$

Next, the preference variation value $\mathfrak{R}v_j$ for each criterion was determined using Eq. 5.

$$[\mathfrak{R}v_j]_9 = \begin{vmatrix} 0.0185 & 0.0177 & 0.0040 & 0.0516 & 0.4478 & 0.0028 & 0.6150 & 0.4239 & 0.0161 \end{vmatrix}$$

For example, it can be determined for the first, second, and last criteria as follows:

$$[\mathfrak{R}_{v_1}] = (1.000 - 0.913)^2 + (0.949 - 0.913)^2 + \dots + (0.851 - 0.913)^2 = 0.0815$$

$$[\mathfrak{R}_{v_2}] = (0.848 - 0.924)^2 + (0.885 - 0.924)^2 + \dots + (0.990 - 0.924)^2 = 0.0177$$

⋮

$$[\mathfrak{R}_{v_9}] = (0.842 - 0.901)^2 + (0.856 - 0.901)^2 + \dots + (0.910 - 0.901)^2 = 0.0161$$

$$[\Psi_j]_9 = \left| \begin{matrix} 0.1326 & 0.1327 & 0.1345 & 0.1281 & 0.0746 & 0.1347 & 0.0520 & 0.0778 & 0.1329 \end{matrix} \right|$$

After that, the index value (Φ_i) of the composite alternatives was calculated using Eq. 8 and is listed in Table 3. For example, the Φ_i can be determined for the first, second, and last alternatives as follows:

$$\Phi_1 = (1.000 \times 0.1326) + (0.848 \times 0.1327) + \dots + (0.842 \times 0.1329) = 0.8494$$

$$\Phi_2 = (0.949 \times 0.1326) + (0.885 \times 0.1327) + \dots + (0.856 \times 0.1329) = 0.7725$$

⋮

$$\Phi_7 = (0.851 \times 0.1326) + (0.990 \times 0.1327) + \dots + (0.910 \times 0.1329) = 0.7948$$

Finally, the overall alternatives were ranked in descending order based on the index values given in Table 3. Table 3 shows that the index value of A-5 is maximum (0.8680), which shows that it is the best among all the available alternatives. While alternatives A-2 and A-3 are showing the least preferences with index values of 0.7725 and 0.7838, respectively. From the results, it can be inferred that as the 60–120 mesh-sized WS content increases from 2.5 wt.% in A-2 to 20 wt.% in A-5, the overall performance generally improves. The samples with identical WS-loadings of different-sized fibers (A-4, A-6, A-7) exhibited rather similar index values.

4 Conclusions

Using agricultural waste to develop polymer composites offers low-cost, sustainable, and viable alternatives for various applications. In the present study, PP-based

Next, the deviation (η_j) was computed in \mathfrak{R}_j using Eq. 6.

$$[\eta_j]_9 = \left| \begin{matrix} 0.9815 & 0.9823 & 0.9960 & 0.9484 & 0.5522 & 0.9972 & 0.3850 & 0.5761 & 0.9839 \end{matrix} \right|$$

Next, the overall preference value (Ψ_j) was determined for each criterion using Eq. 7.

composites were produced using WS waste as filler material. Seven different composites were fabricated using particles of three different mesh sizes (18–35 mesh, 35–60 mesh, and 60–120 mesh) of WS with varying weight proportions (0, 2.5, 5, 10, and 20 wt.%). The properties, such as density, water absorption, tensile, and impact strength, were best for neat PP, while poor for WS-containing composites. However, an enhancement of ~18% in tensile modulus, ~9% in flexural stress at conventional deflection, and ~40% in flexural modulus was recorded for the 60–120 mesh-sized WS-filled (20 wt.%) composite (A-5) compared to neat PP (A-1). The evaluated physical and mechanical properties showed a dependence on the size and quantity of WS, making the composite selection process a cumbersome task. Therefore, the evaluated physical and mechanical properties, material cost, and carbon footprint were fixed as criteria in the composite selection. The preference selection index technique was employed to deal with the selection problem of WS-filled PP composites. Consequently, 20 wt.% of 60–120 mesh-sized WS-filled PP composite was considered the best candidate under the given alternatives and criteria. The proposed decision-making approach could be implemented in various product design and development elements. The study can be extended by adding different compositions, properties (such as chemical, dynamic mechanical, thermal), and decision-making techniques that remain in scope for future study.

Acknowledgements The authors are grateful to MOL Petrochemicals Co. Ltd. for providing the polypropylene used in this study. The authors are grateful to Mikó Stroh Borotai-Laska Ltd. for providing the chopped wheat straw.

Author contribution Each author participated sufficiently in the work. LL and FI produced the samples. LL and FI conducted the tests. LL, SKJ, and TS performed the evaluation of the data. LL and TS wrote the main manuscript text. All authors reviewed the manuscript.

Funding Open access funding provided by Széchenyi István University (SZE). The project was supported by the National Talent Programme (Hungary) through the project NTP-NFTÖ-21-B. Project no. TKP2021-NKTA-48 has been implemented with the support provided by the Ministry of Innovation and Technology of Hungary from the National Research, Development and Innovation Fund.

Data availability The data are available from the first (TS) and the corresponding (LL) authors upon reasonable request.

Table 3 The index values (Φ_i) and ranks of the composite alternatives

Alternatives	$\Phi_i = \sum_{j=1}^m (\delta n_{ij} \times \Psi_j)$	Rank
A-5	0.8680	1
A-1	0.8494	2
A-7	0.7948	3
A-4	0.7923	4
A-6	0.7904	5
A-3	0.7838	6
A-2	0.7725	7

Declarations

Ethical approval Not applicable.

Competing interests The authors declare no competing interests.

Open Access This article is licensed under a Creative Commons Attribution 4.0 International License, which permits use, sharing, adaptation, distribution and reproduction in any medium or format, as long as you give appropriate credit to the original author(s) and the source, provide a link to the Creative Commons licence, and indicate if changes were made. The images or other third party material in this article are included in the article's Creative Commons licence, unless indicated otherwise in a credit line to the material. If material is not included in the article's Creative Commons licence and your intended use is not permitted by statutory regulation or exceeds the permitted use, you will need to obtain permission directly from the copyright holder. To view a copy of this licence, visit <http://creativecommons.org/licenses/by/4.0/>.

References

- Calabi-Floody M, Medina J, Suazo J, Ordiqueo M, Aponte H, Mora MDLL, Rumpel C (2019) Optimization of wheat straw co-composting for carrier material development. *Waste Manag* 98:37–49
- Jiang D, Jiang D, Lv S, Cui S, Sun S, Song X, He S, Zhang J (2021) Effect of modified wheat straw fiber on properties of fiber cement-based composites at high temperatures. *J Market Res* 14:2039–2060
- Bhattacharyya P, Bisen J, Bhaduri D, Priyadarsini S, Munda S, Chakraborti M, Adak T, Panneerselvam P, Mukherjee AK, Swain SL, Dash PK, Padhy SR, Nayak AK, Pathak H, Kumar S, Nimbrayan P (2021) Turn the wheel from waste to wealth: economic and environmental gain of sustainable rice straw management practices over field burning in reference to India. *Sci Total Environ* 775:145896
- Pang B, Zhou T, Cao X-F, Zhao B-C, Sun Z, Liu X, Chen Y-Y, Yuan T-Q (2022) Performance and environmental implication assessments of green bio-composite from rice straw and bamboo. *J Clean Prod* 375:134037
- Yaashikaa PR, Senthil Kumar P, Varjani S (2022) Valorization of agro-industrial wastes for biorefinery process and circular bioeconomy: a critical review. *Biores Technol* 343:126126
- Peidayesh H, Mosnáčková K, Špitalský Z, Heydari A, Šišková AO, Chodák I (2021) Thermoplastic starch-based composite reinforced by conductive filler networks: physical properties and electrical conductivity changes during cyclic deformation. *Polymers (Basel)* 13:3819
- Väisänen T, Haapala A, Lappalainen R, Tomppo L (2016) Utilization of agricultural and forest industry waste and residues in natural fiber-polymer composites: a review. *Waste Manage* 54:62–73
- Lendvai L, Omastova M, Patnaik A, Dogossy G, Singh T (2023) Valorization of waste wood flour and rice husk in poly(lactic acid)-based hybrid biocomposites. *J Poly Environ* 31:541–551
- Dogossy G, Czigany T (2011) Thermoplastic starch composites reinforced by agricultural by-products: properties, biodegradability, and application. *J Reinf Plast Compos* 30:1819–1825
- Masłowski M, Miedzianowska J, Strzelec K (2017) Natural rubber biocomposites containing corn, barley and wheat straw. *Polym Testing* 63:84–91
- Berthet MA, Angellier-Coussy H, Chea V, Guillard V, Gastaldi E, Gontard N (2015) Sustainable food packaging: valorising wheat straw fibres for tuning PHBV-based composites properties. *Compos A Appl Sci Manuf* 72:139–147
- Ahankari SS, Mohanty AK, Misra M (2011) Mechanical behaviour of agro-residue reinforced poly(3-hydroxybutyrate-co-3-hydroxyvalerate), (PHBV) green composites: a comparison with traditional polypropylene composites. *Compos Sci Technol* 71:653–657
- Berthet MA, Gontard N, Angellier-Coussy H (2015) Impact of fibre moisture content on the structure/mechanical properties relationships of PHBV/wheat straw fibres biocomposites. *Compos Sci Technol* 117:386–391
- Mu B, Tang W, Liu T, Hao X, Wang Q, Ou R (2021) Comparative study of high-density polyethylene-based biocomposites reinforced with various agricultural residue fibers. *Ind Crops Prod* 172:114053
- Pan M-Z, Zhou D-G, Bousmina M, Zhang SY (2009) Effects of wheat straw fiber content and characteristics, and coupling agent concentration on the mechanical properties of wheat straw fiber polypropylene composites. *J Appl Polym Sci* 113:1000–1007
- Várdai R, Lummerstorfer T, Pretschuh C, Jerabek M, Gahleitner M, Bartos A, Móczó J, Anggono J, Pukánszky B (2021) Improvement of the impact resistance of natural fiber-reinforced polypropylene composites through hybridization. *Polym Adv Technol* 32:2499–2507
- Lendvai L (2021) A novel preparation method of polypropylene/natural rubber blends with improved toughness. *Polym Int* 70:298–307
- Selvam A, Mayilswamy S, Whenish R, Naresh K, Shanmugam V, Das O (2022) Multi-objective optimization and prediction of surface roughness and printing time in FFF printed ABS polymer. *Sci Rep* 12:16887
- Singh T (2021) Utilization of cement bypass dust in the development of sustainable automotive brake friction composite materials. *Arab J Chem* 14:103324
- Albert FA, Jafrey DJD, Karthik Pandiyan G, John IW, Hariharan S, Guna A, Haribaskar L, Sathish KG, Mohanraj C (2023) Tribological studies and optimization of two-body abrasive wear of NaOH-treated vachellia farnesiana fiber by additive ratio assessment method. *J Mater Eng Perform* 32:82–90
- Mastura MT, Sapuan SM, Mansor MR, Nuraini AA (2018) Materials selection of thermoplastic matrices for 'green' natural fibre composites for automotive anti-roll bar with particular emphasis on the environment. *Int J Precis Eng Manuf-Green Technol* 5:111–119
- Singh T (2021) A hybrid multiple-criteria decision-making approach for selecting optimal automotive brake friction composite. *Mater Des Process Commun* 3:e266
- Yadav AK, Srivastava R (2020) Selection of teak sawdust polypropylene composite's composition for outdoor applications using TOPSIS analysis. *Sādhanā* 45:231
- Singh T (2021) Optimum design based on fabricated natural fiber reinforced automotive brake friction composites using hybrid CRITIC-MEW approach. *J Market Res* 14:81–92
- Haoues S, Yaltese MA, Belhadi S, Chihaoui S, Uysal A (2023) Modeling and optimization in turning of PA66-GF30% and PA66 using multi-criteria decision-making (PSI, MABAC, and MAIRCA) methods: a comparative study. *Int J Adv Manuf Technol* 124:2401–2421
- Lendvai L, Ronkay F, Wang G, Zhang S, Guo S, Ahlawat V, Singh T (2022) Development and characterization of composites produced from recycled polyethylene terephthalate and waste marble dust. *Polym Compos* 43:3951–3959
- Shmls M, Abed M, Horvath T, Bozsaky D (2022) Multicriteria based optimization of second generation recycled aggregate concrete. *Case Stud Constr Mater* 17:e01447

28. Maniya K, Bhatt MG (2010) A selection of material using a novel type decision-making method: Preference selection index method. *Mater Des* 31:1785–1789
29. Gangwar S, Arya P, Pathak VK (2021) Optimal material selection for ship body based on fabricated zirconium dioxide/silicon carbide filled aluminium hybrid metal alloy composites using novel fuzzy based preference selection index. *SILICON* 13:2545–2562
30. Yadav S, Pathak VK, Gangwar S (2019) A novel hybrid TOPSIS-PSI approach for material selection in marine applications. *Sādhanā* 44:58
31. Chauhan R, Singh T, Thakur NS, Patnaik A (2016) Optimization of parameters in solar thermal collector provided with impinging air jets based upon preference selection index method. *Renew Energy* 99:118–126
32. Tweneboaa Kodua L, Xiao Y, Adjei NO, Asante D, Ofosu BO, Amankona D (2022) Barriers to green human resources management (GHRM) implementation in developing countries Evidence from Ghana. *J Clean Prod* 340:130671
33. Madić M, Antucheviciene J, Radovanović M, Petković D (2017) Determination of laser cutting process conditions using the preference selection index method. *Opt Laser Technol* 89:214–220
34. Singh T, Tejyan S, Patnaik A, Chauhan R, Fekete G (2020) Optimal design of needlepunched nonwoven fiber reinforced epoxy composites using improved preference selection index approach. *J Market Res* 9:7583–7591
35. Dixit S, Yadav VL (2019) Optimization of polyethylene/polypropylene/alkali modified wheat straw composites for packaging application using RSM. *J Clean Prod* 240:118228
36. Wu Y, Wang S, Zhou D, Xing C, Zhang Y, Cai Z (2010) Evaluation of elastic modulus and hardness of crop stalks cell walls by nano-indentation. *Biores Technol* 101:2867–2871
37. Lendvai L, Patnaik A (2022) The effect of coupling agent on the mechanical properties of injection molded polypropylene/wheat straw composites. *Acta TechJaur* 15:232–238
38. Ashori A, Nourbakhsh A (2009) Mechanical behavior of agro-residue-reinforced polypropylene composites. *J Appl Polym Sci* 111:2616–2620
39. Zhang Y, Ghali AE, Li B (2012) Physical properties of wheat straw varieties cultivated under different climatic and soil conditions in three continents. *Am J Eng Appl Sci* 5:98–106
40. Mu B, Wang H, Hao X, Wang Q (2018) Morphology, mechanical properties and dimensional stability of biomass particles/high density polyethylene composites: effect of species and composition. *Polymers (Basel)* 10:308
41. Alsabri A, Tahir F, Al-Ghamdi SG (2021) Life-cycle assessment of polypropylene production in the gulf cooperation council (GCC) region. *Polymers (Basel)* 13:3793
42. Cheng K, Yan M, Nayak D, Pan GX, Smith P, Zheng JF, Zheng JW (2015) Carbon footprint of crop production in China: an analysis of National Statistics data. *J Agric Sci* 153:422–431

Publisher's note Springer Nature remains neutral with regard to jurisdictional claims in published maps and institutional affiliations.